CHIN. PHYS. LETT. Vol. 37, No. 5 (2020) 054302

Three-Dimensional Broadband Acoustic Waveguide Cloak *

Chuan-Jie Hu(胡传捷), Ya-Li Zeng(曾雅丽), Yi-Neng Liu(刘益能), Huan-Yang Chen(陈焕阳)**

Institute of Electromagnetics and Acoustics and Key Laboratory of Electromagnetic Wave Science and Detection Technology, Xiamen University, Xiamen 361005

(Received 29 February 2020)

The propagation of acoustic waves is a fundamental topic in shallow ocean acoustics. We numerically demonstrate a three-dimensional zone of silence consisting of a circular tube with gradient index metamaterials attached to its rigid wall. The cloaking effect is verified by fine agreement with analytical calculations.

PACS: 43.30.+m, 42.79.Ry, 02.60.Cb DOI: 10.1088/0256-307X/37/5/054302

Materials have been used to control wave propagation for centuries. In nature, many animals use relatively simple materials to control waves, such as the melon organ of a dolphin[1] and the reflecting bone "mirror" of a bat.[2] Going back decades, unprecedented properties can be obtained to precisely manipulate waves by designing and employing artificial materials, which are called metamaterials.[3,4] Acoustic metamaterials[4] have shown great functionalities and properties, including sound attenuation,[5] negative refraction,[6–8] noise block,[9] acoustic imaging,[10,11] acoustic diode[12] and many other acoustic devices based on transformation acoustics.[13–15] Recently, soft porous silicone rubber materials have even exhibited a wide range of tunable acoustic indices n (from 1.5 to 25 with respect to water[6,16–17]) by varying the material porosity, which would be very useful in designing various acoustic devices. Moreover, gradient-index materials (GIMs) have drawn a great deal of attention.[18–23] It has been shown that propagation waves (PWs) can be efficiently converted to surface waves (SWs) by employing GIMs.[18] This feature leads to a wide range of novel devices, including asymmetric transmission, mode conversion and waveguide cloak for electromagnetic waves.[19–21] In addition, acoustic waves and water waves follow a similar law, and two-dimensional (2D) waveguide cloaks have also been implemented.[22,23] In the field of acoustics, common pipes, wires, plates and wells are in fact three-dimensional (3D) waveguides. It is therefore desirable to utilize GIMs to design a cylindrical waveguide structure to hide an obstacle with suppressed backscattering.

In this Letter, we demonstrate that by integrating the GIMs into waveguide systems, it is possible to achieve a 3D waveguide cloak to hide an irregular obstacle in a circular tube. Numerical simulations are performed to validate the proposed design and they agree well with the analytical derivation.

We demonstrate our configuration in the schematic diagram in Fig. 1. The proposed structure is a 3D circular waveguide with GIMs attached to its rigid wall. The core media is water of inner radius a, which is coated by a cylindrical layer of GIMs (shown by the regions in Fig. 1(b) with gradual blue color) of a fixed thickness d. The outer boundary is the perfect rigid boundary (PRB). The propagation direction of the incident acoustic wave is along the x-axis, and we apply non-reflecting boundary conditions on both ports of the waveguide. The GIMs generate a gradual phase difference as acoustic waves travel through the waveguide, which can enable a conversion from propagating waves (PWs) to quasi-surface waves (QSWs). The evolution of this process and its inverse eventually create a forbidden region that can be used to hide obstacles.

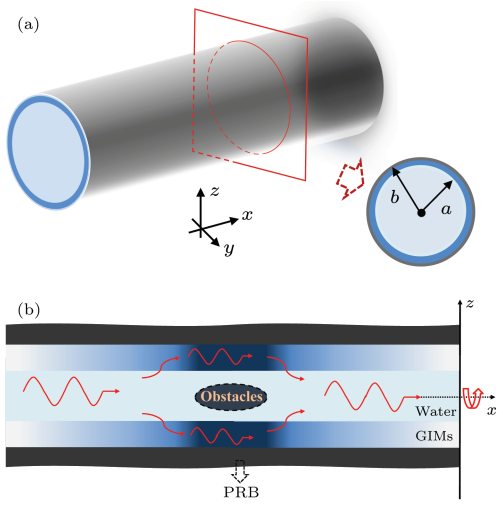

Fig. 1. (a) A schematic plot of a three-dimensional waveguide with GIMs. (b) For the view of x–z section, the waveguide is constructed with GIMs (denoted by the gradually blue regions) attached to the rigid walls (the black region). The background media is water, depicted as light blue region. The red arrows demonstrate the sketchy path of acoustic wave propagation.

The index profiles of GIMs along x direction can

*Supported by the National Natural Science Foundation of China (Grant No. 11874311) and the Natural Science Foundation of Fujian Province, China (Grant No. 2017J05015).

**Corresponding author. Email: kenyon@xmu.edu.cn

© 2020 Chinese Physical Society and IOP Publishing Ltd

be described as

$$n(x)=\begin{cases}1+\frac{k\left(x+\frac{3L}{2}\right)}{2k_0d}, & -\frac{3L}{2}\leqslant x\leqslant -\frac{L}{2},\\ 1+\frac{kL}{2k_0d}, & -\frac{L}{2}\leqslant x\leqslant \frac{L}{2},\\ 1-\frac{k\left(x-\frac{3L}{2}\right)}{2k_0d}, & \frac{3L}{2}\leqslant x\leqslant \frac{L}{2},\end{cases} \tag{1}$$

where k_0 is the wave vector of the background medium (water), k is a crucial momentum parameter, and d is the thickness of the GIMs. Here the waveguide is assumed to be infinite in length with uniform cross section. Thus, we only need to generate transverse finite elements in uniform sections of the waveguide, which significantly reduces the number of degrees of freedom required in finite element simulations (we will use commercial software COMSOL Multiphysics). Let us start from a fixed position and replace the GIMs with a homogeneous material, which has the same parameters as the GIMs at this position. The dispersion relations related to each position of the GIMs can be analytically solved, which helps us to better understand the acoustic wave propagation in the waveguide. In the following theoretical derivation, we assume that the inner media (water) is region 1 and the GIMs are region 2, respectively.

In the time domain, the governing equation of acoustic wave in a circular tube could be described in a cylindrical coordinate system:

$$\frac{1}{r}\frac{\partial}{\partial r}\left(r\frac{\partial p}{\partial r}\right)+\frac{1}{r^2}\frac{\partial^2 p}{\partial\theta^2}+\frac{\partial^2 p}{\partial x^2}=\frac{1}{c^2}\frac{\partial^2 p}{\partial t^2}, \tag{2}$$

where r, θ, x and p are the radial distance, polar angle, tube axial distance and acoustic pressure, respectively.

According to the method of separating variables, supposing the solution is

$$p\left(r,\theta,x,t\right)=R\left(r\right)\Theta\left(\theta\right)X\left(x\right)e^{jwt}. \tag{3}$$

Let us substitute it into Eq. (2), and three ordinary differential equations (ODEs) can be established:

$$\frac{d^2x}{dx^2}+k_x^2X=0, \tag{4}$$

$$\frac{d^2\Theta}{d\theta^2}+m^2\Theta=0, \tag{5}$$

$$\frac{d^2R}{dr^2}+\frac{1}{r}\frac{dR}{dr}+\left(k_r^2-\frac{m^2}{r^2}\right)R=0. \tag{6}$$

After some calculations, we have

$$X\left(x\right)=A_xe^{-jk_xx}, \tag{7}$$

$$\Theta\left(\theta\right)=A_\theta\cos\left(m\theta+\phi_m\right), \tag{8}$$

$$\frac{d^2R}{dg^2}+\frac{1}{g}\frac{dR}{dg}+\left(1-\frac{m^2}{g^2}\right)R=0, \tag{9}$$

where we suppose $g=k_rr$. It is not difficult to find that Eq. (9) is a standard Bessel function of order m, and its general solution can be expressed as

$$R\left(k_rr\right)=A_rJ_m\left(k_rr\right)+B_rN_m\left(k_rr\right). \tag{10}$$

It is worth noting that the second item of pressure in region 1 should be discarded because the Neumann function diverges at zero point and the pressure inside the tube must be finite. The general sound pressure solution of regions 1 and 2 can be written as follows:

$$p_1=AJ_m\left(k_{r1}r\right)\cos\left(m\theta+\phi_m\right)e^{j(\omega t-k_zx)}\ \text{for region 1,} \tag{11}$$

$$p_2=[BJ_m\left(k_{r2}r\right)+CN_m\left(k_{r2}r\right)]\cos\left(m\theta+\phi_m\right)e^{j(\omega t-k_zx)}\ \text{for region 2.} \tag{12}$$

By matching the continual boundary conditions of p and $\frac{1}{\rho_r}\frac{\partial p}{\partial r}$ at $r=a$ and the outer hard boundary condition of $\frac{1}{\rho_r}\frac{\partial p}{\partial r}$ at $r=b$ and assuming that the density of different regions is the same, we have

$$\begin{aligned}&AJ_m\left(k_{r1}a\right)-BJ_m\left(k_{r2}a\right)-CJ_m\left(k_{r2}a\right)=0,\\ &Ak_{r1}J'_m\left(k_{r1}a\right)-Bk_{r2}J'_m\left(k_{r2}a\right)-Ck_{r2}N'_m\left(k_{r2}a\right)=0,\\ &Bk_{r2}J'_m\left(k_{r2}b\right)-Ck_{r2}N'_m\left(k_{r2}b\right)=0.\end{aligned} \tag{13}$$

After a series of calculations and simplifications, the dispersion relation of the waveguide with GIMs at a fixed position can be derived as

$$\frac{k_{r1}J'_m(k_{r1}a)}{k_{r2}J_m(k_{r1}a)}=\frac{J'_m(k_{r2}a)N'_m(k_{r2}b)-N'_m(k_{r2}a)J'_m(k_{r2}b)}{J_m(k_{r2}a)N_m(k_{r2}b)-N_m(k_{r2}a)J'_m(k_{r2}b)}. \tag{14}$$

The wave vectors in the two regions have the relationships $k_{r1}^2=k^2-\beta^2$, $k_{r2}^2=(nk)^2-\beta^2$, where $k=\frac{2\pi f}{c}$, and β is the wave vector in the x direction for the two regions and c is the velocity of acoustic waves in water.

In the simulations, we consider the waveguide with the parameters as follows: $a=22\,\text{cm}$, $b=24\,\text{cm}$, $d=2\,\text{cm}$, $c=1500\,\text{m/s}$ in water, $k=0.2k_0$ and the working frequency is 2250 Hz. The whole length of the waveguide is $3L$, $L=100\,\text{cm}$. The profile of the relative refractive index is from 1 to 6. Inside the waveguide, the obstacles are three irregular scatterers. Each obstacle is a cone formed by an isosceles triangle rotating along the x-axis. The three obstacles are with the same height ($h=36\,\text{cm}$) and the same length ($w=36\,\text{cm}$). For convenience, we only show three refractive indices 1, 2 and 3 to explain the underlying mechanism in Fig. 2. For the incident acoustic wave from the left port, the waveguide is coupled to zero mode, as shown in Figs. 2(a) and 2(d). When it reaches the position where the refractive index is 2, the dispersion curve of zero mode goes below the water line (as shown in Fig. 2(b)). The intensity at the center becomes smaller from the mode pattern. When it reaches the position where the refractive index is 3, there are three branches of dispersion curves under the water line, as shown in Fig. 2(c). However, only the zero mode is excited out here. Moreover, the mode is gradually converted into quasi-surface waves, as depicted in Fig. 2(f). The intensity at the center becomes

near zero and most part is confined in the GIM layer, which would be useful for our further cloaking design. For incident waves with higher-order circular modes, the principle of mode conversion is also applicative.

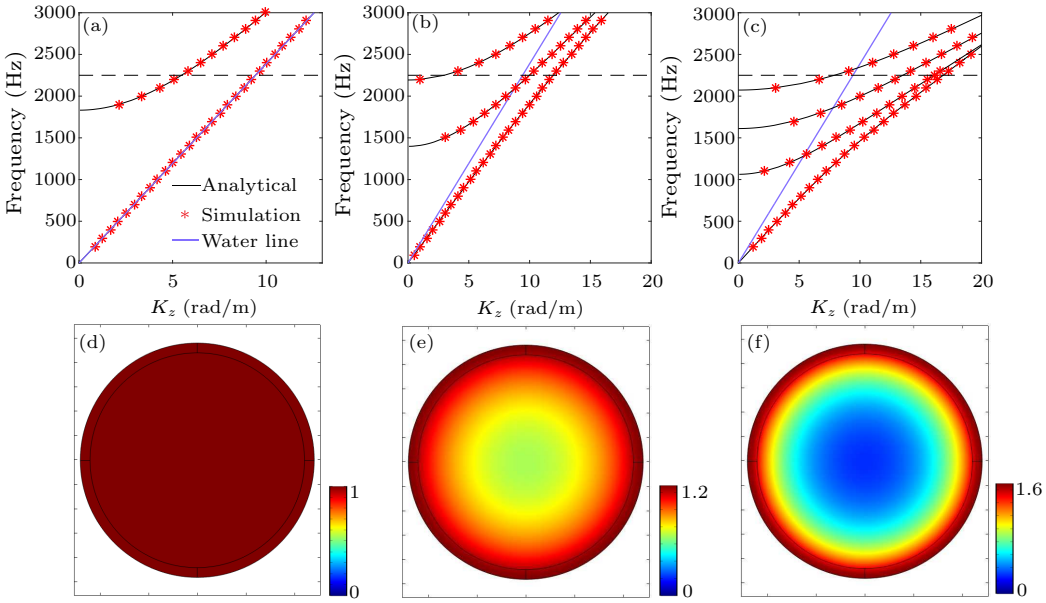

Fig. 2. (a)–(c) Dispersion of the waveguide with the GIMs replaced by three kinds of homogeneous effective media with relative refractive indices: (a) 1, (b) 2, and (c) 3. The black lines indicate the analytical solutions, which agree well with the simulations. The gray line is the water line and the black dashed lines indicate the working frequency 2250 Hz. (d)–(f) The field diagrams of zero mode at the working frequency for effective media with the refractive indices: (d) 1, (e) 2, and (f) 3.

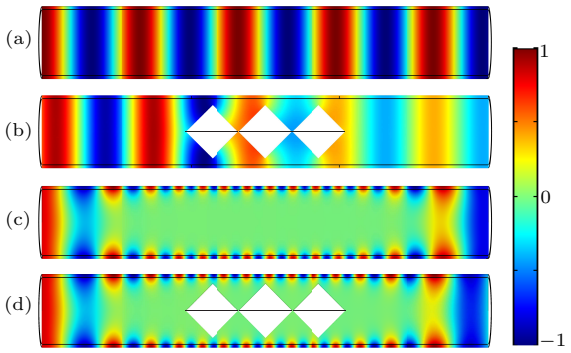

Fig. 3. The proposed 3D waveguide cloak for suppression of backscattering. The simulated pressure field (a) without and (c) with GIMs at 2250 Hz, (b) for an obstacle placed in the center of an empty cylindrical waveguide, and (d) for an obstacle placed in the waveguide with GIMs.

Figures 3(a)–3(d) show the pressure field patterns for an empty cylindrical waveguide, the waveguide with an obstacle, the unloaded cylindrical waveguide cloak and the waveguide cloak for hiding obstacles, respectively. In Fig. 3(a), we demonstrate the propagation of a plane acoustic wave in an empty waveguide at 2250 Hz. If rigid obstacles are put in the middle, then there will be very strong backscattering, as shown in Fig. 3(b) with reflectance 78%. When GIMs are added to the rigid wall of the empty tube, the evolution of zero mode has been illustrated in Fig. 2. From the pressure field in Fig. 3(c), there is a silence region where the amplitude of acoustic waves is extremely weak (nearly zero). Thus, with the help of GIMs attached to the wall, the propagation of the acoustic wave in the waveguide with obstacles is just like that in an unloaded waveguide (as depicted in Fig. 3(d)), with negligible backscattering (reflectance of 2.2%).

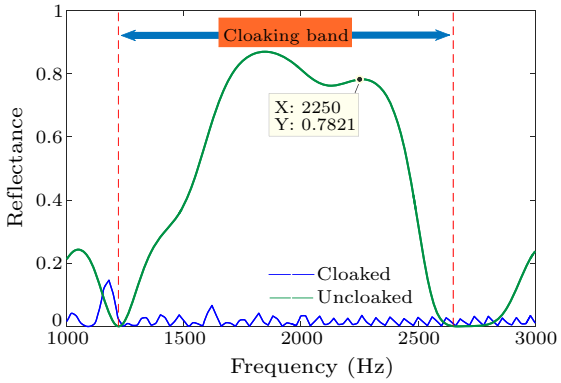

Fig. 4. The reflectance for obstacles in the cloaked (the blue curve) and the uncloaked (the green curve) 3D cylindrical waveguide.

In addition, we plot the reflectance for obstacles in the waveguide without or with GIMs, as shown by the green curve and the blue curve. It can be seen that the cloaking effect is very good in a wide frequency band (from 1220 Hz to 2650 Hz). Figure 4 shows that the reflectance of obstacles in the simulation is as high as 78% and the transmission efficiency is low at 2250 Hz. In the cloaking band, the reflectance of the waveguide cloak with obstacles is almost below 5%. It is noted that there is little backscattering, which results from the crest of the quasi-surface waves partially hindered

by the peaks of obstacles at the center of the waveguide.

In summary, we have demonstrated that a 3D broadband acoustic waveguide cloak can be achieved using a cylindrical waveguide with GIMs attached to its rigid wall. With the rapid development of acoustic metamaterials, this approach is easier to implement than other strategies of cloaking that require materials of high anisotropy, or isotropy but with extreme parameters, or with more space filled with extremely complex structures. In daily life, common pipes, wires and wells are examples of three-dimensional waveguides. Hence, the extension of waveguide cloak and other mode evolution devices to 3D has excellently potential applications. The proposed structure has great significance in the field of acoustic communication and high-efficiency sensors. In addition, the waveguide cloaking effect may find applications in health monitoring of waveguides and non-destructive inspections[24] for cracks in the wall.

Chuan-Jie Hu thanks Dr. Yongdu Ruan for helpful discussion.

References

[1] Dong E, Zhou Y, Zhang Y et al 2020 *Phys. Rev. Appl.* **13** 024002
[2] Zhuang Q and Müller R 2006 *Phys. Rev. Lett.* **97** 218701
[3] Smith D R, Pendry J B and Wiltshire M C K 2004 *Science* **305** 788
[4] Cummer S A, Christensen J and Alù A 2016 *Nat. Rev. Mater.* **1** 16001
[5] Liu Z, Zhang X, Mao Y et al 2000 *Science* **289** 1734
[6] Brunet T, Merlin A, Mascaro B et al 2015 *Nat. Mater.* **14** 384
[7] Li J and Chan C T 2004 *Phys. Rev. E* **70** 055602
[8] Zhu X, Liang B, Kan W et al 2011 *Phys. Rev. Lett.* **106** 014301
[9] Bell J S, Summers I R, Murray A R J et al 2012 *Phys. Rev. B* **85** 214305
[10] Jia H, Ke M, Hao R et al 2010 *Appl. Phys. Lett.* **97** 173507
[11] Cheng Y, Zhou C, Wei Q et al 2013 *Appl. Phys. Lett.* **103** 224104
[12] Liang B, Yuan B and Cheng J 2009 *Phys. Rev. Lett.* **103** 104301
[13] Chen H, Yang T, Luo X et al 2008 *Chin. Phys. Lett.* **25** 3696
[14] Chen H and Chan C T 2007 *Appl. Phys. Lett.* **91** 183518
[15] Cummer S A and Schurig D 2007 *New J. Phys.* **9** 45
[16] Brunet T, Leng J and Mondain-Monval O 2013 *Science* **342** 323
[17] Ba A, Kovalenko A, Aristégui C et al 2017 *Sci. Rep.* **7** 1
[18] Xu Y, Fu Y and Chen H 2016 *Nat. Rev. Mater.* **1** 16067
[19] Xu Y, Gu C, Hou B et al 2013 *Nat. Commun.* **4** 2561
[20] Wang H X, Xu Y D, Genevet P et al 2016 *Sci. Rep.* **6** 24529
[21] Gu C, Xu Y, Li S et al 2015 *Sci. Rep.* **5** 12106
[22] Zou S, Xu Y, Zatianina R et al 2019 *Phys. Rev. Lett.* **123** 074501
[23] Cao W K, Wu L T, Zhang C et al 2019 *Sci. Bull.* **64** 808
[24] Shah H, Balasubramaniam K and Rajagopal P 2017 *J. Phys. Commun.* **1** 055004